ARTICLE
Journal of Cellular Biochemistry 116:67–80 (2015)

Journal of Cellular Biochemistry

Glucose Availability and Glycolytic Metabolism Dictate Glycosphingolipid Levels

Morgan Stathem,[1] Subathra Marimuthu,[1] Julie O'Neal,[2] Jeffrey C. Rathmell,[3] Jason A. Chesney,[1,2,4] Levi J. Beverly,[1,2,4]* and Leah J. Siskind[1]**

[1]*Department of Pharmacology and Toxicology, University of Louisville School of Medicine, Louisville Kentucky*
[2]*James Graham Brown Cancer Center, University of Louisville, Louisville Kentucky*
[3]*Department of Pharmacology and Cancer Biology, Duke University, Durham North Carolina*
[4]*Division of Hematology and Oncology, Department of Medicine, University of Louisville School of Medicine, Louisville Kentucky*

ABSTRACT

Cancer therapeutics has seen an emergence and re-emergence of two metabolic fields in recent years, those of bioactive sphingolipids and glycolytic metabolism. Anaerobic glycolysis and its implications in cancer have been at the forefront of cancer research for over 90 years. More recently, the role of sphingolipids in cancer cell metabolism has gained recognition, notably ceramide's essential role in programmed cell death and the role of the glucosylceramide synthase (GCS) in chemotherapeutic resistance. Despite this knowledge, a direct link between these two fields has yet to be definitively drawn. Herein, we show that in a model of highly glycolytic cells, generation of the glycosphingolipid (GSL) glucosylceramide (GlcCer) by GCS was elevated in response to increased glucose availability, while glucose deprivation diminished GSL levels. This effect was likely substrate dependent, independent of both GCS levels and activity. Conversely, leukemia cells with elevated GSLs showed a significant change in GCS activity, but no change in glucose uptake or GCS expression. In a leukemia cell line with elevated GlcCer, treatment with inhibitors of glycolysis or the pentose phosphate pathway (PPP) significantly decreased GlcCer levels. When combined with pre-clinical inhibitor ABT-263, this effect was augmented and production of pro-apoptotic sphingolipid ceramide increased. Taken together, we have shown that there exists a definitive link between glucose metabolism and GSL production, laying the groundwork for connecting two distinct yet essential metabolic fields in cancer research. Furthermore, we have proposed a novel combination therapeutic option targeting two metabolic vulnerabilities for the treatment of leukemia. J. Cell. Biochem. 116: 67–80, 2015.

KEY WORDS: SPHINGOLIPID; GLUCOSE; CERAMIDE; GLYCOSPHINGOLIPID; GSL; GLUCOSYLCERAMIDE; GlcCer; GluCer; GLUCOSYLCERAMIDE SYNTHASE; GCS; GLYCOLYSIS; PENTOSE PHOSPHATE PATHWAY; PPP; METABOLISM; APOPTOSIS; 2-DEOXYGLUCOSE; 2-DG; 6-AMINONICATINOMIDE; 6-AN; ABT-263; ABT-737

The role of glycolytic metabolism in cancer has been extensively studied since Otto Warburg published his landmark theory on aerobic glycolysis in tumor cells over 80 years ago. The "Warburg Effect" states that cancer cells take up increased glucose compared to their non-transformed counterparts and preferentially utilize glycolytic metabolism to produce ATP, even in the presence of oxygen, a phenomenon termed aerobic glycolysis [Warburg, 1956]. Enigmatically, however, the alternative energetic pathway, oxidative phosphorylation, produces significantly more ATP than aerobic glycolysis per molecule of glucose. This begs the question: why do cancer cells preferentially utilize glycolysis, which is a "less efficient" pathway? Increased glycolytic metabolism is utilized to provide the raw materials needed for rapid growth in the form of anaplerotic substrates. These substrates are produced through

The authors declare no conflicts of interest.

Grant sponsor: National Institutes of Health; Grant number: NCRR P20 RR17677 COBRE; Grant sponsor: NIDDK; Grant number: R01 DK093462; Grant sponsor: James Graham Brown Cancer Center; Grant sponsor: Kosair Pediatric Oncology Research Program.

*Correspondence to: Levi J. Beverly, Department of Medicine, James Graham Brown Cancer Center, University of Louisville, 505 S. Hancock St., rm. 204, Louisville, KY 40202, USA. E-mail: Levi.Beverly@Louisville.edu
**Correspondence to: Leah J. Siskind, Department of Pharmacology and Toxicology, University of Louisville School of Medicine, 505 S. Hancock St., rm. 203. Louisville, KY 40202, USA. E-mail: leah.siskind@Louisville.edu

Manuscript Received: 18 June 2014; Manuscript Accepted: 15 August 2014
Accepted manuscript online in Wiley Online Library (wileyonlinelibrary.com): 21 August 2014
DOI 10.1002/jcb.24943 • © 2014 Wiley Periodicals, Inc.

shuttling of glycolytic pathway intermediates into a variety of additional metabolic pathways, such as the pentose phosphate pathway (PPP), the tricarboxylic acid (TCA) cycle, nucleotide biosynthesis and glycogen synthesis [DeBerardinis et al., 2007, 2008; Vander heiden et al., 2009; Dang, 2012]. While increased glycolytic flux has previously been tied to the production of substrates for a myriad of anabolic reactions, one such area has been largely unexplored, that of glycosphingolipid metabolism.

Sphingolipids are bioactive lipid molecules involved in both regulation of membrane dynamics and intracellular signaling. Among the cellular functions in which sphingolipids participate, the best characterized is their role in programmed cell death, or apoptosis. Treatment of cancer cells with chemotherapeutics elevates levels of the pro-apoptotic sphingolipid ceramide in a multitude of cancer cell lines during mitochondrial induced cell death [Haimovitz-Friedman et al., 1997; Pettus et al., 2002]. In fact, generation of ceramide is a prerequisite for many mechanisms of apoptotic cell death [Jean-Philippe and Filippo, 2003; Siskind et al., 2010], and reduction of cellular ceramide via metabolism to other sphingolipid members is observed in drug-resistant cells [Itoh et al., 2003; Gouaze-Andersson and Cabot, 2006]. Glucosylceramide (GlcCer) is generated through the addition of UDP-glucose to ceramide by the enzyme glucosylceramide synthase (GCS) and is the precursor molecule for a vast network of complex glycosphingolipids (GSLs) (a simplified overview of sphingolipid metabolism is outlined in Fig. 1). GSLs themselves are associated with anti-apoptotic, pro-proliferative phenotypes in a variety of disease states [Chatterjee and Wei, 2003; Gouaze-Andersson and Cabot, 2006]. Elevated levels of GCS and GlcCer are widely implicated in multi-drug resistance (MDR) in many cancers [Gouaze-Andersson et al., 2007; Liu et al., 2013]. Furthermore, tumor cells have distinct GSL profiles compared to non-transformed cells [Nohara et al., 1998], a phenotype associated with aberrant cell–cell adhesion and intracellular signaling, which play a significant role in tumor cell progression, metastasis, and response to treatment [Hakomori and Zhang, 1997]. Therefore, GCS has been an attractive target for the development of anti-cancer pharmaceuticals as both a primary treatment and a combinatorial treatment with cytotoxic therapies for the treatment of drug-resistant malignancies [Chai et al., 2011].

Given that GCS utilizes UDP-glucose to generate GlcCer, it would follow that increased glucose availability might elevate GSL levels. Indeed, work in diabetic models does indicate a correlation between glucose uptake and GSL production. In a mouse model of type 1 diabetes mellitus (DM1), both UDP-glucose [Needleman et al., 1968]

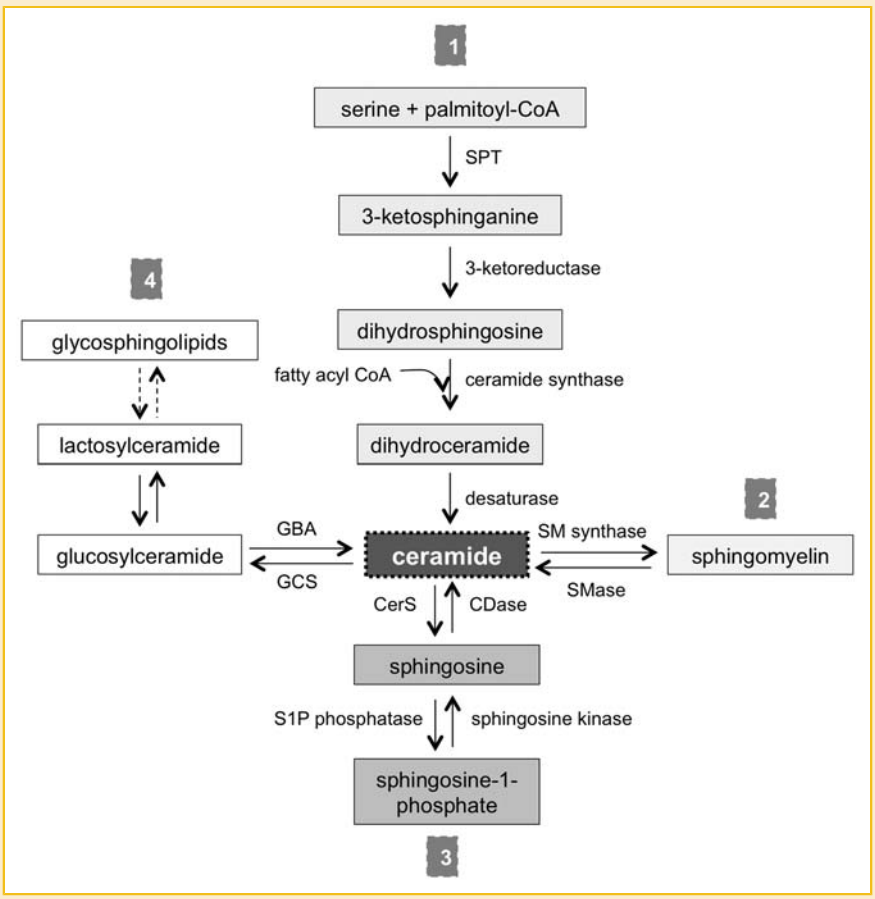

Fig. 1. An overview of sphingolipid metabolism. Formation of ceramide occurs through the de novo pathway (1), SM hydrolysis pathway (2), sphingomyelinase arm of the salvage pathway (3), or β-glucocerebrosidase (GBA) arm of the salvage pathway (4). The ratio of ceramide to glucosylceramide is an important factor in the survival of cells. Glucosylceramide is formed through addition of UDP-glucose to ceramide by glucosylceramide synthase (GCS) or the breakdown of lactosylceramide.

and glycosphingolipid levels are elevated in the kidney in response to increased plasma concentrations of glucose [Zador et al., 1993; el-Khatib et al., 1996]. Conversely, inhibition of GSL production via GCS improves glucose tolerance in animal models of DM1 [Zhao et al., 2007]. Furthermore, reduction of GSL levels via inhibition of GCS increases both glucose uptake and glycolytic metabolism in leukemia cells [Ji et al., 1998], suggesting a compensatory mechanism by which the cell restores GSL levels through increased uptake and metabolism of the requisite substrates. Although these studies establish a connection between glucose availability, substrate production and GSL levels, they are inherently confounded by either: (1) the presence of disease states, for which the presence of external variables cannot be excluded or (2) the aberrant signaling pathways characteristic of transformed cells which undoubtedly influence glycolytic metabolism beyond glucose uptake.

Despite the fact that increased glucose availability is a hallmark of most cancers and elevated GSLs are widely accepted as a prognostic marker of cancer progression and metastatic potential, an objective relationship between the two has yet to be drawn. Herein, we have established a link between the distinct, yet clearly interrelated metabolic fields of glycolytic and GSL metabolism. We demonstrate that increasing glucose uptake in a non-transformed cell line is sufficient to increase the GSL levels. Alternatively, withdrawing glucose from these same cells causes a dramatic depletion in total GSL levels. We provide evidence to show that in the absence of aberrant intracellular signaling, this effect is mainly a substrate driven process. Furthermore, inhibition of both glycolysis and the PPP with targeted inhibitors 2-DG and 6-AN, respectively, depletes GSL levels in the same model. We also present findings that this link persists in hematological malignancies and that inhibition of glycolytic and PPP metabolism influences GSL levels therein. Finally, we show that in a leukemia cell model, metabolic inhibitors 2-DG and 6-AN synergize with pro-apoptotic BCL-2 inhibitor ABT-263 in inducing apoptosis. Overall, these data demonstrate a clear link between glucose uptake and utilization and the production of GSLs.

MATERIALS AND METHODS

CELL CULTURE AND REAGENTS

FL5.12 WT and HG cells were kindly provided by Dr. Jeffrey Rathmell (Duke University Medical Center, Durham, NC) [Rathmell et al., 2003]. Human leukemia cells were purchased from ATCC. All cells were maintained in HyClone RPMI 1640 (Thermo Scientific #SH 30027) medium containing 10% FBS supplemented with 2 mM L-Glutamine, 10 mM HEPES (Gibco 15630–80) and 1× pen-strep (Gibco 15140-122); FL5.12 cells were additionally supplemented with 2 ng/ml recombinant mouse IL-3 and 1× β-mercaptoethanol. FL5.12 cells were maintained in the log growth phase between 5×10^5 and 2×10^6 c/ml. Leukemia cells were maintained in the log growth phase between 1×10^5 and 2×10^6 c/ml.

CELL VIABILITY ASSAY

Cells growing in the log phase were seeded in 96- well dishes (2,500 FL5.12, U937, or 5,000 OCI AML 3 or 7,500 K562 cells per well) and immediately treated with the indicated drug concentrations in a total volume of 200 μl per well. All treatments were done in triplicate. 2-DG (#14325) and 6-AN (#10009315) were obtained from from Cayman and ABT-263 (cat#CT-A263) from Chemietek (Indianapolis, IN). Cells were incubated for 48 h and 10% (20 μl) Alamar Blue reagent (cat#DAL1100) from Invitrogen (Grand Island, NY) was added. Plates were then further incubated for 4 h and the fluorescence of Alamar Blue reduction was determined on a BioTek HT Synergy plate reader (540 nm excitation, 594 nm emission). Wells containing only complete RPMI media and vehicle plus 20 μl of Alamar Blue were averaged and subtracted from all experimental readings. Drug treatment regimens were then normalized to either vehicle treated cells or to wells containing only the IC_{30} of the indicated drug. Each graph shown is a representative experiment of at least three biological replicates.

WESTERN BLOT ANALYSIS

5×10^6 cells were harvested and lysed in 350 μl of RIPA lysis buffer (NEBL #9806S) via sonication for 30 s. Protein concentrations were determined using BCA protein assay reagent from Pierce (#23223 and #23224). 40 μg of total protein was used for standard Western blot procedure. Samples were boiled at 98° for 5 min before being run on SDS-PAGE gel (BioRad #345-0033) and transferred using the iBlot Transfer System (Novex). Membranes were blocked in TBS-T with 5% milk for 1 h at room temperature. Primary antibody was added in the following dilutions: 1:1,000 anti-GLUT1 (Santa Cruz #SC-7903), 1:2,500 anti-HK1 (Cell Signaling #2024); 1:10,000 anti-actin (Sigma #A5441), 1:10,000 anti-tubulin (Sigma #T5168). Anti-mouse and anti-rabbit were added at a dilution of 1:10,000. Chemiluminescent detection was performed using Pierce ECL Western Blot Substrate (#32106) from Thermo Scientific according to manufacturer's protocol.

INTRACELLULAR LIPID MEASUREMENT

5×10^6 cells were seeded in 10 cm dishes containing complete RPMI without antibiotics and treated with the indicated drug(s) or appropriate vehicle in biological triplicates. At the indicated times, cells were harvested, washed two times in 5 mL of ice cold PBS, then cell pellets were snap frozen in liquid nitrogen. Quantification of sphingolipid species was performed by the Lipidomics Core Facility at the Medical University of South Carolina (MUSC) on a Thermo Finnigan TSQ 7000, triple-stage quadrupole mass spectrometer operating in a Multiple Reaction Monitoring (MRM) positive ionization mode as described [Bielawski et al., 2006]. Excess lipids were obtained and extracted using the Bligh and Dyer method. Data were normalized to either total lipid phosphate or cell number, as indicated.

IN SITU GLUCOSYLCERAMIDE SYNTHASE ACTIVITY ASSAY

5 mg NBD-C_6-Ceramide complexed with BSA (Life Technology #N22651) was dissolved in 150 μl sterile dH_2O (0.5 mM NBD-C_6-Ceramide and 0.5 mM BSA) and stored at −20°C. 1×10^6 cells were plated in a 6-well plate in 2 ml of complete RPMI 1640 media. 20 μM PDMP was added to the appropriate wells; remaining cells received DMSO as vehicle. Cells were incubated for 2 h at 37°C. All cells then received 2 μM of NBD-C_6-Ceramide and were incubated at 37 °C for

30 min. Cells were collected, spun at 1,000×g for 5 min at 4 °C, and supernatant was removed. Cells were washed 1× by adding ice-cold PBS (1,000×g, 5 min, 4 °C). Supernatant was removed. Lipids were extracted by Bligh and Dyer method [Presley et al., 1993]. Briefly, cells were resuspended with 260 μl of ice-cold PBS and transferred to glass tubes. 666 μl of methanol was added to the cells and vortexed 2 × 30 s. Cells were then kept on ice for 10 min. 333 μl of chloroform and 333 μl of water was added to tubes, which were vortexed two times for 30 s then spun at 3,000 rpm for 5 min at room temperature. The lower phase (containing the lipids) was transferred to a new set of glass tubes and lipids were dried down by nitrogen gas. Lipids were then resuspended in 30 μl of chloroform/methanol (2:1 v/v) and loaded onto HP-TLC plates (Millipore #1.05644.0001) for separation. NBD-glycosphingolipids were used as standards. The chromatogram was developed in a solvent system consisting of chloroform/methanol/30%ammonium hydroxide/water (350:150:18:7 by volume). TLC plates were scanned on a BioRad phosphorimager. Band density was quantified by Quantity One software (count/mm^2). NBD-GlcCer are normalized to total (NBD-Ceramide + NBD-GlcCer), and the normalized to total cell number and time.

QUANTITATIVE REAL-TIME REVERSE TRANSCRIPTION PCR

Total RNA was extracted using EZNA Total RNA Kit I (OMEGA biotek #R6834) according to the manufacturer's protocol. The concentration and quality of total RNA preparations were evaluated by NanoDrop. cDNA was synthesized from 1 ug of total RNA using the iScript cDNA Synthesis Kit for first-strand synthesis (BioRad # 170-8890). Quantitative real-time PCR (qPCR) was performed on a Bio-Rad CFX96 Real-Time detection system using SsoFast EvaGreen Supermix (BioRad # 172-5202). Standard reaction volume was 25 μl containing 12.5 μl Supermix, 9.5 μl dH_2O (Sigma), 400 nM specific oligonucleotide primers, and 25 ng of cDNA template. β-Actin was used as reference gene. Reaction was carried out as follows for UGCG, GBA, and β-actin: enzyme activation 95 °C, 30 s; denaturation 95 °C, 5 s; annealing 60 °C 5 s; 40 cycles total. Primers were validated for temperature and efficiency prior to use in qPCR. Primer sequences are as follows:

hACTB: ATTGGCAATGAGCGGTTCC (F), GGTAGTTTCGTGGATGCCACA (R)

hUGCG: GAATGGCCGTCTTCGGGTT (F), AGGTGTAATCGGGTGTAGATGAT (R)

hGBA: CCGATGGCTCTGCTGTTGTG (F), CAGGTAGGTGTGAATGGAGTAGC (R)

mACTB: AGATTACTGCTCTGGCTCCTAG (F), CCTGCTTGCTGATCCACATC (R)

mUGCG: CCTTGTTCGGCTTCGTGCTCTTC (F), TGCTATACGGCTGTTTGTCTGTTGC (R)

mGBA: TGGATGCTTATGCTAAGTATGG (F), CACGGGAAATGAAGTCTCTCTG (R)

GLUCOSE UPTAKE

1×10^6 cells were plated in glucose-free RPMI 1640 media supplemented with 10% dialyzed FBS. Cells were incubated for 30 min to allow equilibration with media. Following incubation, cells were given 25 μl of ^{14}C deoxy-glucose (0.1 μCi/μl) for 1 h, then washed three times with ice cold PBS. Cells were lysed in 500 μl 0.1% SDS. 400μl of lysate was added to 5 ml Microscint 40 scintillation fluid (Perkin Elmer) and counts were measured on a Tri-Carb 2910 liquid scintillation analyzer (Perkin Elmer). Remaining lysate was quantitated with the BCA Assay as described above. Counts were normalized to μg protein concentration.

STATISTICAL ANALYSIS

A one-way ANOVA with Halm-Sidak posttest was used for samples $n > 2$. A two-tailed t-test was used for samples where $n = 2$. Unless otherwise indicated: all data points represent the compilation of at least three biological triplicates; data are represented as average ±SD; dose-response graphs are a representative graph of an experiment conducted in triplicate; * $P < 0.05$.

RESULTS

GLUCOSE AVAILABILITY DICTATES GLYCOSPHINGOLIPID LEVELS IN HIGHLY GLYCOLYTIC CELLS

To determine whether glucose availability in and of itself is sufficient to drive GSL production, we utilized the IL-3 dependent FL5.12 hematopoietic progenitor cell line over-expressing glucose transporter Glut-1 and the rate-limiting glycolytic enzyme HK-1 (herein FL5.12 HG) [Rathmell et al., 2003] (Fig. 2A). This cell line represents a model of highly glycolytic cells independent of the intracellular or extracellular aberrations observed in disease states. As expected, FL5.12 HG cells took up 83-fold more glucose as compared to their wild-type counterparts (Fig. 2B). Furthermore, over-expression of HK1 in HG cells led to a significant decrease in sensitivity to treatment with the HK-1 competitive inhibitor 2-DG ($IC_{50} = 0.33$ mM vs 1.7 mM for wild-type and HG, respectively) (Fig. 2C). This was further confirmed by treatment of both cell lines with a single dose 2-DG and determination of relative cell viability. At 1 mM of 2-DG the cell growth of wild-type cells was inhibited by 65%, whereas HG cells were inhibited only 27% (Fig. 2D).

Previous studies indicated that increased glucose availability resulted in increased GSL levels in DM1 mice [Zador et al., 1993]. Therefore, we assessed if the same phenomenon would occur in our model of highly glycolytic cells. Indeed, increased glucose availability resulted in elevated GSL levels in HG cells compared to wild-type (Fig. 3A). This led us to question whether glucose withdrawal would correspondingly decrease GlcCer levels. Indeed, wild-type cells withdrawn from glucose for 18 h showed a marked decrease in GlcCer levels compared to cells continuously cultured in glucose (Fig. 3B). To investigate the extent to which glucose availability impacts enzymatic GlcCer formation, we measured the expression and activity of GCS and β-Glucocerebrosidase (GBA), the enzymes responsible for the anabolic and catabolic formation of GlcCer, respectively. Although GlcCer levels were dramatically elevated in HG cells over wild-type, increased glucose availability did not significantly alter the expression of GCS or GBA (Fig. 3C). Moreover, GCS activity did not increase over wild-type in HG cells (Fig. 3D). Collectively, these data indicate that glucose availability plays a role in controlling GSL levels. Furthermore, in non-transformed cell lines increased GSL production appears to be a

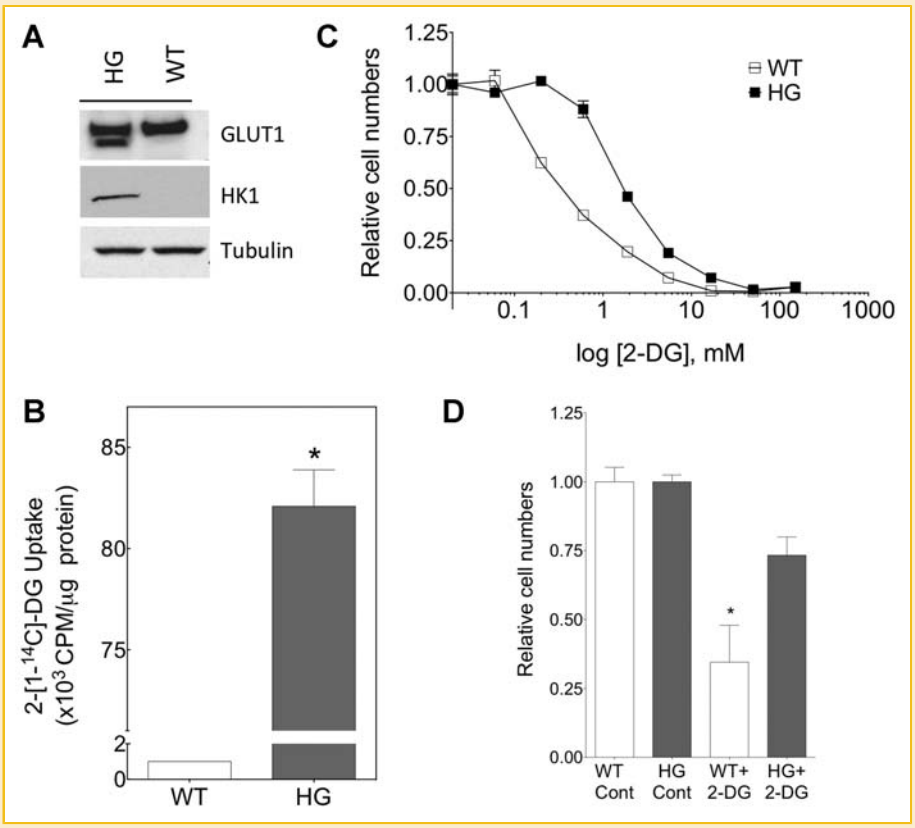

Fig. 2. FL5.12 cells overxpressing GLUT1 and HK1 are highly glycolytic. (A) FL5.12 HG cells stably overexpress glycolytic enzymes GLUT1 and HK1. Overexpression of integral membrane protein GLUT1 and HK1 was confirmed by Western blot. HK1 is not endogenously expressed in wild-type FL5.12 cells. GLUT1 was overexpressed in the pSFFV vector using rat GLUT1 cDNA. Rat and mouse GLUT1 proteins have slightly different molecular weights due to variations in their amino acid sequence, thus ran at different apparent molecular weights on SDS page gel and present as separate bands. (B) FL5.12 WT and HG cells were grown in glucose-free media for 1 h, incubated with 14C 2-D-deoxy-glucose for 1 h, then collected and counted by scintillation. FL5.12 HG cells took up significantly more glucose than their WT counterparts. (C) Relative cell viability as a function of 2-DG treatment. Cells were treated for 48 h with 2-DG (0.06–150 mM) FL5.12, then measured for cell viability via AlamarBlue reduction. HG cells are more resistant to treatment with HK-1 competitive inhibitor 2-DG vs wild-type cells ($IC_{50} = 0.33$ mM vs 1.7 mM for wild-type and HG, respectively, at 48 h). (D) FL5.12 cells were treated for 48 h with 1 mM 2-DG and cell viability was measured using AlamarBlue reagent. Wild-type cells are significantly more sensitive to 2-DG treatment than HG cells (65% reduction in cell viability vs 27% in wild-type and HG, respectively). Graph B represents duplicate samples, $n = 2$.

substrate driven process relatively independent of GCS expression or activity.

INHIBITORS OF GLYCOLYTIC METABOLISM AND THE PENTOSE PHOSPHATE PATHWAY DECREASE GLYCOSPHINGOLIPID LEVELS

Given that glucose availability plays a clear role in GSL formation (Figs. 2B and 3A), we determined whether selective inhibition of the rate-limiting enzymes of bioenergetic pathways downstream of glucose uptake would decrease GSL levels. To this effect, we utilized 2-DG, a glycolytic inhibitor which targets hexokinase and 6-AN, a PPP inhibitor which targets glucose-6-phosphate dehydrogenase (G6PD). FL5.12 cells were treated in a dose response manner with 2-DG (Fig. 2C) or 6-AN (data not shown) to establish the respective IC_{50} of each cell line for these inhibitors. WT and HG cells were then treated for 8 h with 2-DG IC_{50} or 6-AN IC_{50} and total hexosylceramide (glucosyl- and galactosylceramide) levels were measured via HPLC-MS/MS. As shown in Fig. 4, hexosylceramide levels significantly decreased following treatment with 2-DG in both WT and HG cells. Treatment with 6-AN significantly decreased hexosylceramide levels in WT cells, however this effect was blunted in HG cells (mean overall decrease of 24% vs 7%, respectively). It should be noted, however, that specific chain lengths of hexosylceramides, namely C16 and C22, significantly decreased in response to 6-AN treatment in HG cells.

Overall, these data support the hypothesis that GSL levels are at least in part influenced by the production of substrates produced via glycolysis and the PPP.

GLYCOSPHINGOLIPID LEVELS IN LEUKEMIA CELLS ARE PRIMARILY DICTATED BY GCS ACTIVITY

FL5.12 HG cells provided an excellent, syngeneic in vitro model for establishing a relationship between increased glucose availability and GSL production; however, inherently lacked the aberrations in intracellular signaling present in cancer cells. In order to determine if this relationship persisted in neoplastic cells, we utilized four leukemia and lymphoma cell lines (collectively "leukemia" cell lines for simplicity), U937, OCI AML3, RAJI, and HEL (Fig. 5A). Baseline GlcCer levels were measured via HPLC-MS/MS. GlcCer levels were

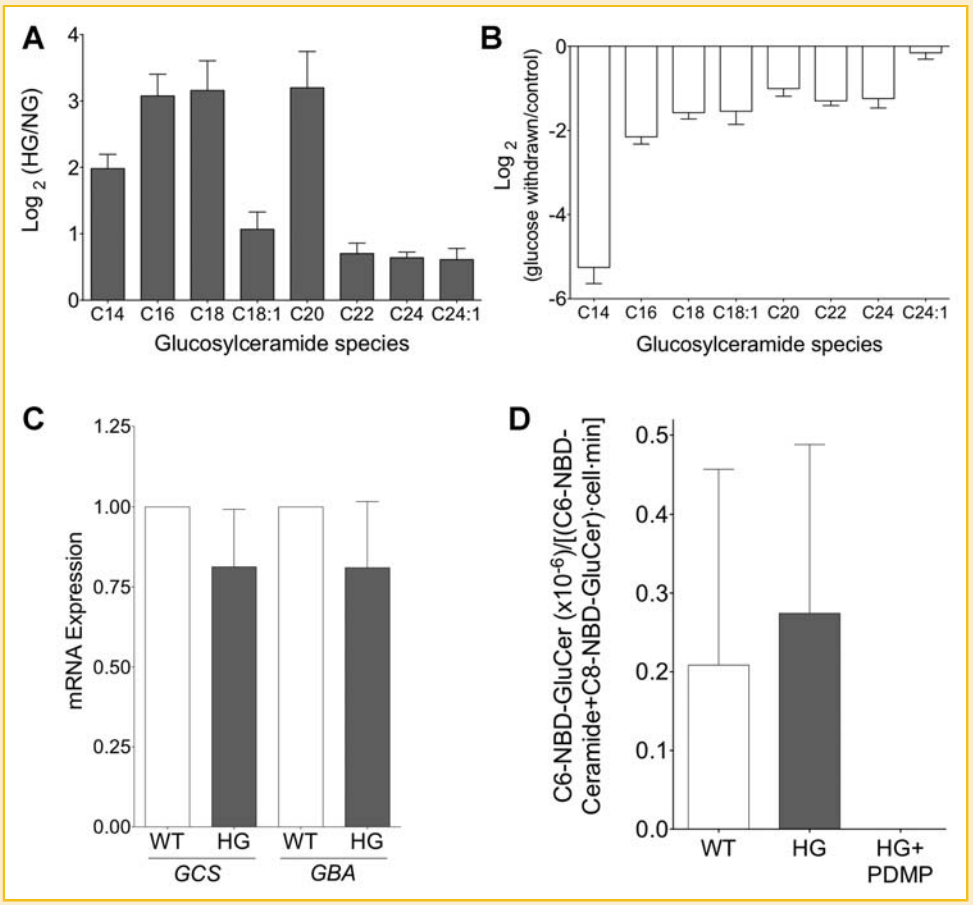

Fig. 3. Glucosylceramide levels are elevated in a model of highly glycolytic cells. (A,B) Total cellular glucosylceramide levels were measured via HPLC-MS/MS. (A) FL5.12 HG cells, normalized to wild-type FL5.12 cells, were determined by HPLC-MS/MS. FL5.12 HG cells show an increase in both short-chain and long-chain glucosylceramide levels. (B) FL5.12 wild-type cells were cultured in the absence of glucose for 18 h and the total amount of cellular glucosylceramides was determined by HPLC-MS/MS. Glucose withdrawal markedly decreased glucosylceramide levels as compared to non-glucose withdrawn cells. (C) FL5.12 cells were grown for 24 h in complete media then analyzed for expression of GCS and GBA via qPCR. WT expression was set to 1.0 and HG expression was normalized to wild-type. GCS and GBA expression decreased compared to wilt-type cells. (D) GCS activity was measured in FL5.12 wild-type and HG cells. Cells were grown in complete media for 2 h, then measured for GCS activity via addition of NBD-ceramide and separation on TLC. GCS activity in HG cells was slightly elevated compared to wild-type. Addition of PDMP to HG cells ablated GCS activity, as expected. Graphs B and D represent duplicate samples, n = 2.

elevated in U937 and OCI AML3 cell lines and decreased in RAJI and HEL, when compared to cultured, proliferating human cord blood CD34+ cells (Fig. 5B). Given that increased glucose availability correlated with increased GlcCer levels in our model of highly glycolytic FL5.12 cells, we examined whether leukemia cells with elevated GlcCers also took up more glucose. Indeed, U937 and OCI AML3 cells took up elevated, albeit non-significant amounts, of glucose compared to RAJI and HEL cells (Fig. 5C).

To elucidate the extent to which glucose availability correlates with enzymatic GlcCer production in these cell lines, we again measured GCS expression and activity. Similar to FL5.12 cells, there was no significant change in the mRNA expression of either GCS or GBA across the leukemia cell lines (Figs. 6A and 6B). In contrast to FL5.12 cells, however, GlcCer levels positively correlated with GCS activity in our panel of leukemia cells, in that cell lines with elevated GlcCer (U937 and OCIAML3) had increased GCS activity compared to those with low GlcCer levels (RAJI and HEL) (Fig. 6C). Collectively, these results suggest that increased GlcCer levels in leukemia cell lines may be primarily influenced by increased GCS activity. Glucose availability may also influence baseline GlcCer levels in some leukemia cells, perhaps through the production of substrates formed during and downstream of glucose metabolism.

INHIBITORS OF GLYCOLYTIC METABOLISM AND THE PENTOSE PHOSPHATE PATHWAY SYNERGIZE WITH ABT-263 TO INCREASE CERAMIDE:GLYCOSPHINGOLIPID RATIOS

Anti-apoptotic BCL-2 family proteins are upregulated in many cancers, especially leukemias [Placzek et al., 2010]. We have shown previously that that PDMP, an inhibitor of GCS activity, sensitizes U937 cells to treatment with ABT-263, a small molecule inhibitor of anti-apoptotic BCL-2 family proteins Bcl-2, BCL-xL, and Bcl-w [Casson et al., 2013]. To evaluate whether inhibition of the proposed metabolic pathways upstream of GSL formation also synergize with ABT-263 to kill leukemia cells, we tested the combination of 2-DG or

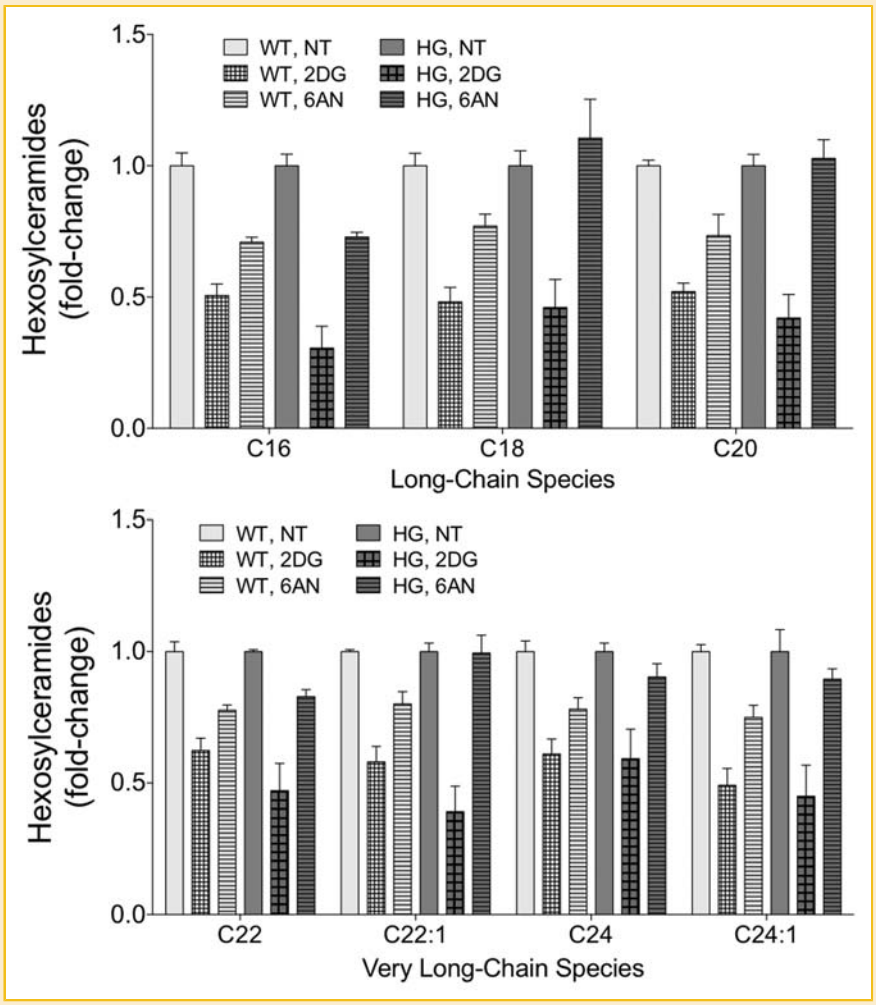

Fig. 4. Inhibition of FL5.12 cells with metabolic inhibitors depletes GSLs. FL5.12 WT and HG cells were treated with 2-DG IC_{50} (0.5 mM vs 1.5 mM for WT and HG, respectively) or 6-AN IC_{50} (4.5 μM vs 3 μM for WT and HG, respectively) for 8 h. Total hexosylceramide levels were determined via HPLC-MS/MS and normalized to cell number. Long-chain ceramides (C16-C20) and very long chain hexosylceramides (C22+) are shown. 2-DG significantly decreased all hexosylceramide chain lengths in WT and HG cells, albeit a 10% greater decrease was observed in HG cells (45% vs 56%, respectively). 6-AN significantly decreased hexosylceramide levels of all species in WT cells, however only C16 and C22 hexosylceramides were depleted in HG cells.

6-AN with ABT-263 in U937 cells. Cells were treated in a dose-response manner for 48 h, either with increasing doses of 2-DG and the IC_{30} ABT-263 or vice versa (Fig. 7A). The same treatment pattern was followed using 6-AN and ABT-263 (Fig. 7C). The presence of 2-DG or 6-AN significantly decreased the dose of ABT-263 required to induce cell death. The IC_{50} for ABT-263 alone was 5 μM, however upon addition of 2-DG decreased 12.5-fold to 0.4 μM, and decreased even more dramatically in combination with 6-AN, from 5 μM to 0.15 μM, a 37-fold reduction. The same phenomenon was observed when ABT-263 was added at a constant dose to increasing doses of 2-DG or 6-AN (Figs. 7B and D), reducing the IC_{50} by 14- and 18-fold, respectively.

If 2-DG and 6-AN blocked metabolic pathways necessary for the production of requisite GlcCer substrates, then treatment of cells with these inhibitors should cause a significant decrease in the total levels of GlcCer. Ceramide, GlcCer, and lactosylceramide levels were measured via HPLC-MS/MS following treatment for 8 h with 2-DG, 6-AN, and ABT-263 alone or in combination. Increases in intracellular ceramide are a hallmark of apoptotic cell induction [Haimovitz-Friedman et al., 1997; Pettus et al., 2002]. Indeed, following treatment with ABT-263, which induces cell death through induction of mitochondrial-induced apoptosis, ceramide levels significantly increased (Figs. 8A and B). Furthermore, upon addition of 2-DG (Fig. 8A) or 6-AN (Fig. 8B), ceramide levels synergistically increased compared to ABT-263 alone. As expected, 2-DG or 6-AN alone did not significantly increase ceramide levels, given that at low concentrations they inhibit cell growth rather than induce apoptosis [Pelicano et al., 2006]. Notably, however, 2-DG and 6-AN caused a dramatic drop in GlcCer levels by 45% and 23%, respectively, a decrease further augmented by addition of ABT-263 (an additional 20% and 40%, respectively) (Fig. 8). The role of lactosylceramide in cell death is not as clear; however, it is worth noting that treatment with 6-AN, not 2-DG, decreased lactosylceramide levels, as well (Fig. 8).

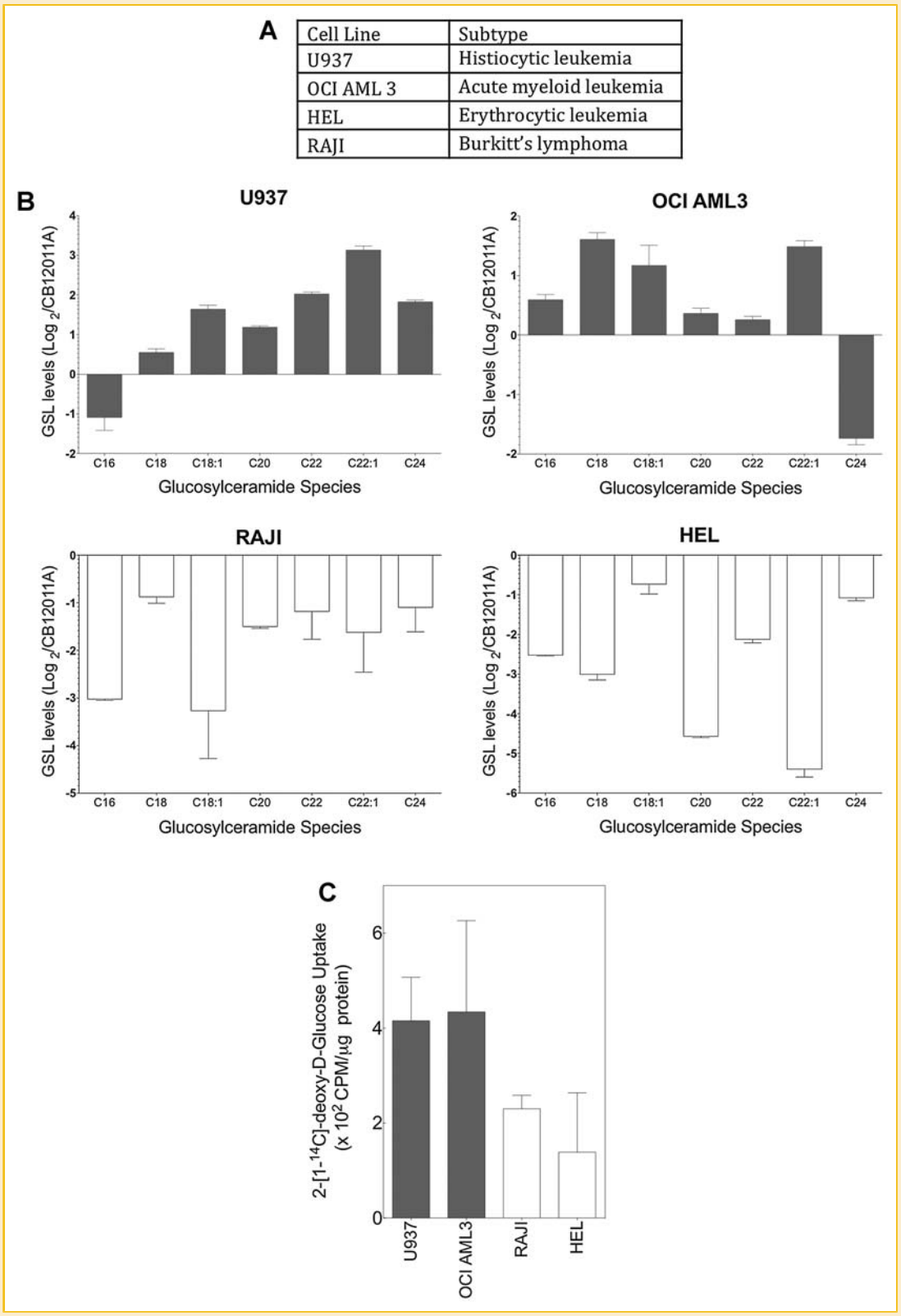

Fig. 5. Glucosylceramide levels differ among a panel of leukemia cell lines. (A) Leukemia cell lines used in the present study. (B) Total cellular glucosylceramide levels were measured by HPLC-MS/MS and normalized to cord blood cell line CB12011A. Glucosylceramide levels were elevated in U937 and OCI AML three cell lines and decreased below baseline in RAJI and HEL cell lines. Levels of glucosylceramides correlated with glucose uptake in the leukemia cells. (C) Glucose uptake was measured in four leukemia cell lines. Cells were grown in serum-free glucose-free media for 1 h, incubated with 14C 2-D-deoxy-glucose for one hour, then collected and counted by scintillation. Glucose uptake is shown as absolute values. U937 and OCI AML3 took up more, although not significant, levels of glucose compared to RAJI and HEL cells.

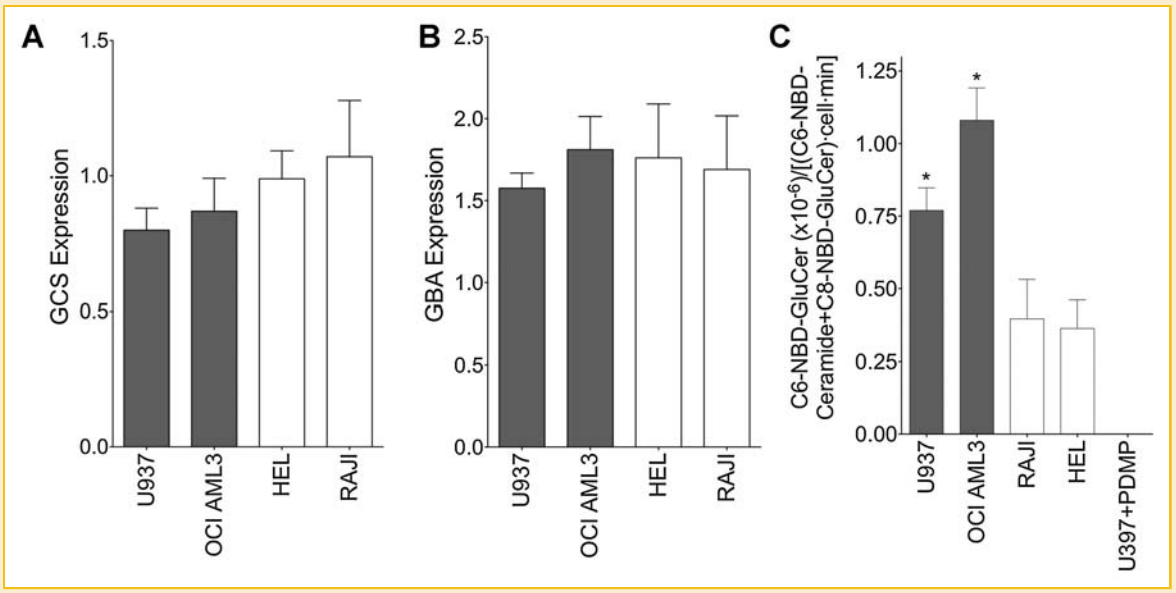

Fig. 6. GCS activity is increased in leukemia cell lines with elevated glucosylceramides. (A, B) Leukemia cells were cultured in complete media for 24 h and then analyzed for expression of GCS and GBA by qPCR. (A) Levels of GCS mRNA were slightly (though non-significantly) decreased in high GluCer cells vs low GluCer cells (U937 and OCI AML3 vs RAJI and HEL, respectively). (B) GBA Mrna expression was not significantly different among the part of leukemia cells. (C) GCS activity was measured in leukemia cells. Cells were grown in complete media for 2 h, then analyzed for GCS activity via addition of NBD-ceramide and separation by TLC. GCS activity was significantly elevated in high GlcCer cells compared to low GlcCer cells (U937, OCI AML 3 vs RAJI, HEL, respectively). Addition of PDMP to U937 cells ablated GCS activity, as expected.

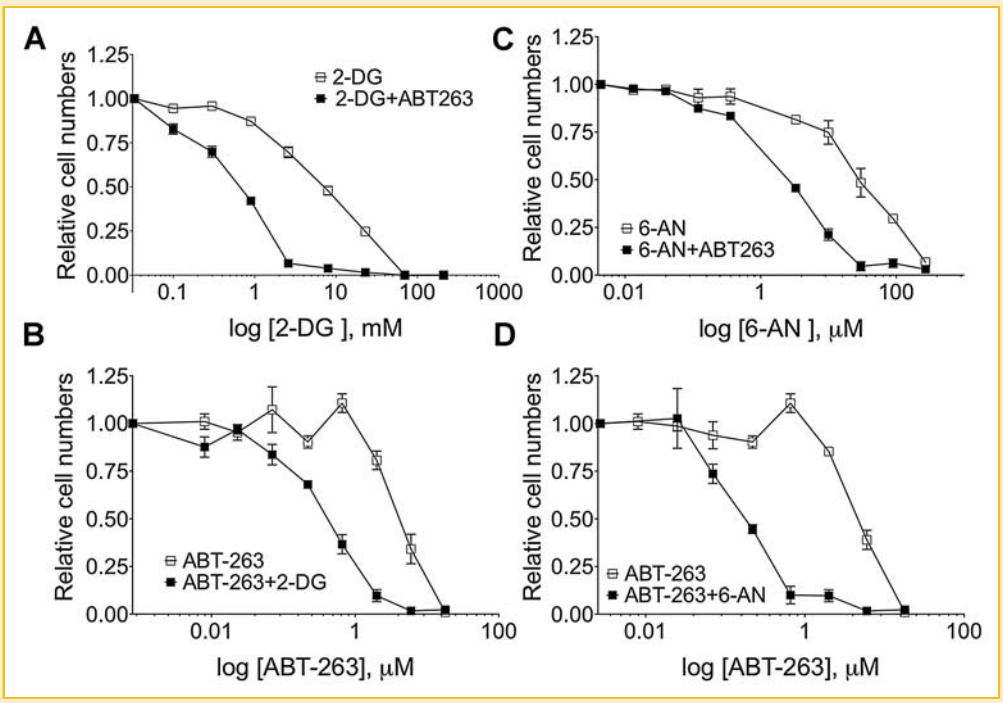

Fig. 7. Inhibitors of glycolytic metabolism and the PPP synergize with an inhibitor of anti-apoptic BCL2 proteins. (A,B) 2-DG synergizes with ABT-263 in killing U937 cells. U937 cells were incubated for 48 h with (A) increasing doses of 2-DG plus either vehicle or ABT-263 IC_{30} (5 μM) or (B) increasing doses of ABT-263 plus vehicle or IC_{30} 2-DG (1.7 mM) for 48 h. The relative number of viable cells was determined using reduction of AlamarBlue reagent. (C,D) U937 cells were incubated for 48 h with (C) increasing doses of 6-AN plus vehicle or IC_{30} (5 μM) of ABT-263 or (D) increasing doses of ABT-263 plus vehicle or the IC_{30} of 6-AN for 48 h. Cell viability was determined using reduction of AlamarBlue reagent. Doses: 2-DG: 33 μM to 170 mM; 6-AN: 13.3 nM to 170 μM; ABT-263: 2.7 nM to 18 μM.

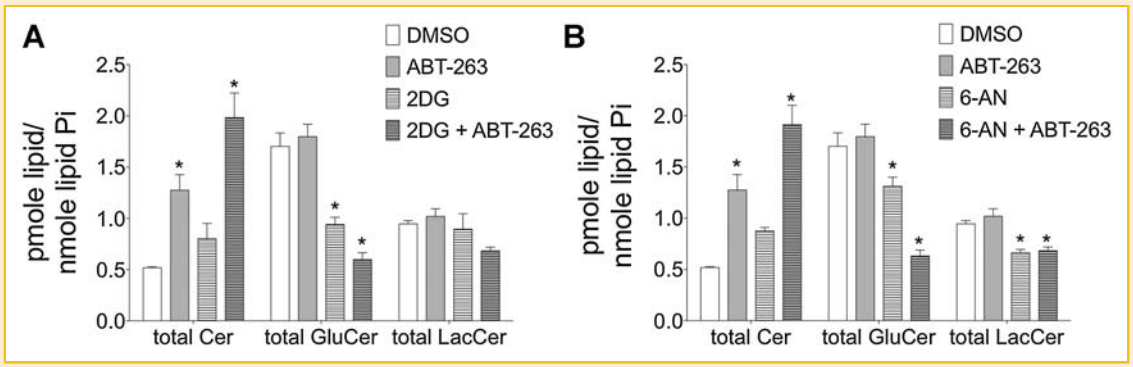

Fig. 8. Inhibitors of glycolytic metabolism and the PPP synergize with an inhibitor of anti-apoptotic BCL2 proteins to increase ceramide:glycosphingolipid ratios. (A) U937 cells were treated with vehicle (DMSO), ABT-263 IC_{30} (5 μM), 6-AN IC_{30} (1.7 μM), or the combination of 6-AN and ABT-263 at their respective IC_{30}. (B) U937 cells were treated vehicle (DMSO), ABT-263 IC_{30}, 2-DG IC_{30}, or the combination of 6-AN and ABT-263 at their respective IC_{30}. Treatment with ABT-263 significantly increases ceramide levels but does not decrease glucosyl- or lactosylceramide levels. Treatment with 6-AN and 2-DG increase ceramide levels slightly, though not significantly, but do cause a significant decrease in glucosylceramide levels. Treatment with ABT-263 in combination with 2-DG or 6-AN causes a significant augmentation of ceramide levels over ABT-263 alone and significantly decreases glucosylceramide levels over 2-DG or 6-AN alone. 6-AN, but not 2-DG, significantly decreases lactosylceramide levels. All data points represent the compilation of three biological triplicates.

These data further support the hypothesis that both glycolysis and the PPP are instrumental in providing substrates for GlcCer formation. Furthermore, nutrient deprivation via metabolic inhibition synergizes with ABT-263 in inducing cell death via ceramide accumulation within the cell, data which is consistent with many other studies showing that metabolic inhibition of cancer cells primes for cell death induction via cytotoxic inhibitors [Maschek et al., 2004; Dwarakanath, 2009; Aghaee et al., 2012].

DISCUSSION

A limited amount of data exists linking glucose availability to the production of GSLs, the seminal work performed by the Shayman group [Zador et al., 1993; el-Khatib et al., 1996] in rat models of DM1. Furthermore, this association has never been shown outside of a metabolic disease state or in neoplastic cells. In the present study we have shown that there exists a definitive link between glucose availability and GSL formation, independent of aberrant intracellular signaling pathways or the influence of the extracellular environment of disease states. Glucose transporter 1 (GLUT1) and Hexokinase II (HK2) are often overexpressed in response to oncogenic signaling pathways to support the increased reliance on aerobic glycolysis [Pedersen et al., 2002; Macheda et al., 2005]. Accordingly, many cancers, solid tumors and blood cancers inclusive, take up elevated amounts of glucose and thus can be considered highly glycolytic [Warburg, 1956; Hsu and Sabatini, 2008; Lunt and Vander Heiden, 2011]. Our model of highly glycolytic cells, FL5.12 HG, overexpressed both Glut-1 and HK2 in a non-transformed hematopoietic cell line (Fig. 2A), which increased glucose uptake (Fig. 2B) and significantly elevated GlcCer levels (Fig. 3A). On the other hand, glucose withdrawal in wild-type FL5.12 cells correspondingly decreased GlcCer levels below baseline levels of non-withdrawn cells (Fig. 3B). Interestingly, C14 showed a markedly stronger decrease upon glucose deprivation compared to other species. Extensive data suggests that ceramide-derived species of varying fatty acyl chain lengths have unique roles in cellular processes [Mullen et al., 2011; Grosch et al., 2012; Hartmann et al., 2013]. Given that glucose withdrawal has been shown to induce autophagy [Jones, 2009], a process which ceramide has been shown to play a key role in [Grosch et al., 2012], it is possible that either C14-GlcCer is a negative regulator of autophagy and was thus decreased, or a product downstream of its degradation positively regulates this process. Overall, these data support our hypothesis that glucose availability in and of itself can directly influence GSL levels. We found that this is primarily a substrate-driven process, given that neither expression nor activity of GCS, the enzyme responsible for GlcCer formation, was significantly altered between the two cell lines (Figs. 3C and D).

Leukemia and lymphoma are umbrella classifications for complex and heterogeneous groups of bone marrow- and lymphatic-derived malignancies, respectively, each with its own unique aberrations in cellular signaling and metabolic profiles. As such, we chose to study the relationship between glucose metabolism and GSL levels irrespective of genetic background in a panel of leukemia and lymphoma cell lines (U937, OCI AML3, RAJI, HEL) (Fig. 5B). Given that cancer cells are already highly glycolytic in nature, it is not surprising that a significant difference in glucose uptake was not observed between the leukemia cell lines and that GlcCer levels are not entirely dependent on its uptake (Fig. 5C), although from the data it could be inferred that differential uptake may play a role. On the other hand, we found that GCS activity is significantly increased in cell lines with elevated GlcCer levels. This is in contrast to FL5.12 HG cells, in which glucose uptake directly corresponded to GlcCer levels, without significantly altering GCS expression or activity. Overall, these data indicate that other mechanisms may be at play in transformed cells in addition to regulation of substrate uptake and GCS enzyme expression. As the following data would indicate, this may be related to shunting of glucose into pathways essential for GlcCer and GSL production in cell lines with elevated GSL levels.

GCS catalyzes the formation of GlcCer from ceramide and UDP-glucose, suggesting that GlcCer levels may be influenced by glucose availability and that inhibition thereof would deplete its levels. Indeed, inhibition of glycolysis with 2-DG significantly depleted GSLs in WT FL5.12 cells, even more so in their HG counterparts (Fig. 4). Interestingly, targeting the PPP with 6-AN also significantly depleted GSLs in WT cells, however had very little effect in HG cells. We propose this discrepancy is the product of heterogeneous degrees of glucose uptake and the effects of targeting different stages of metabolism downstream thereof. Inhibition with 2-DG blocks glycolysis and all biosynthetic pathways downstream of glucose-6-phosphate, including the PPP, TCA cycle, fatty acid synthesis, and glycogen synthesis (see Fig. 9 for schematic). As such, both WT and HG cells would theoretically experience the same level of substrate depletion at their respective IC_{50}. On the other hand, 6-AN preferentially targets the PPP, leaving other biosynthetic avenues open to produce the substrates needed to maintain elevated GSL levels. Due to the marked increase in glucose uptake in HG cells, blockade of the PPP may drive excess metabolites into other pathways and thus provide the requisite substrates for GSL synthesis.

In contrast to our non-transformed highly glycolytic model, one of the main advantages of aerobic glycolysis in neoplastic cells is the production of intermediates for shunting into anaplerotic pathways to support a requisite increase in biomass. We hypothesized that one such biosynthetic pathway supported by this metabolic transformation is GSL synthesis, given the essential role of GSLs both in membrane composition [Lingwood, 2011] and tumor progression [Hakomori, 1996; Liu et al., 2013]. Consistent with our findings in non-transformed cells, 2-DG significantly depleted overall GSL levels in U937 cells (Fig. 8A). On the other hand, 6-AN caused a significant, albeit less marked as compared to 2-DG, decrease in GSL levels in this cell line (Fig. 8B). Overall these results suggest that in neoplastic cells, elevated glucose uptake may increase flux into pathways downstream of glycolysis provide the requisite substrates for production of GSLs.

In the present study we have provided strong evidence correlating glucose availability and GSL synthesis: (1) increased glucose uptake leads to increased GSL levels; (2) glucose withdrawal depletes GSL levels; and (3) inhibition of metabolic pathways such as glycolysis and the PPP reduce GSL levels in both non-transformed and transformed cell lines. On the basis of the following observations, we hypothesize that in addition to producing intermediates for biosynthetic reactions which fuel the highly proliferative state of cancer cells, formation of these substrates also serves to increase the production of GSLs via GCS. An overview of the proposed mechanism is provided in Figure 9. Briefly, through shunting into the PPP, glucose provides intermediates such as ribose-5-phosphate for synthesis of nucleotides such as UTP. Furthermore, glucose-6-phosphate may in turn be metabolized to glucose-1-phosphate, which is combined with UTP to form UDP-glucose (releasing PP_i). In support of this mechanism, evidence has shown that increased glucose uptake also leads to increased flux into glycogen synthesis [Kroemer and Pouyssegur, 2008], which is elevated both at baseline and in response to external stress in the neoplastic cell [Cori and Cori, 1925; Tsavachidou et al., 2010; Iida et al., 2012]. Furthermore, increased glucose availability has been previously shown to increase intracellular UDP-glucose levels in the kidney in rat models of diabetes [Needleman et al., 1968; Spiro, 1984], an increase which

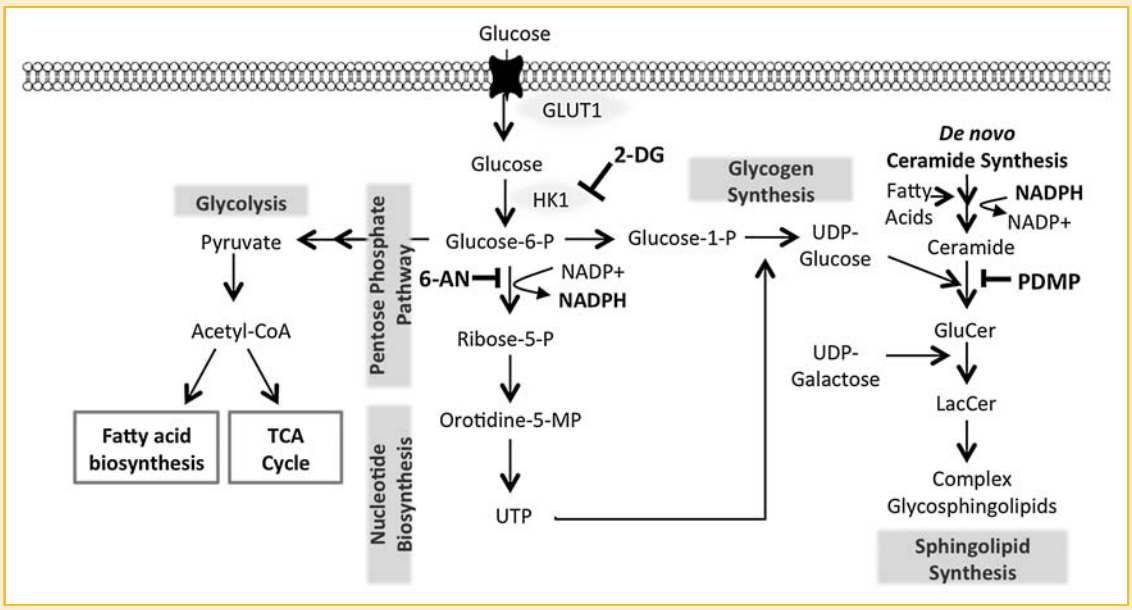

Fig. 9. Schematic representation for the proposed mechanism of glycosphingolipid production via formation of substrates from glycolysis and the PPP in highly glycolytic cells. Certain leukemia cells take up elevated levels of glucose, leading to increased flux through glycolysis and into the pentose phosphate pathway, glycogen synthesis, nucleotide biosynthesis, and the TCA cycle. We hypothesize that increased flux into these pathways leads to the production of the rate-limiting substrates necessary for glycosphingolipid formation, namely, fatty acyl CoA, UDP-glucose, and NADPH. Inhibitors used in the present study are shown in red and enzymes overexpressed in the FL5.12 cell line are highlighted in yellow.

was later shown to elevate GSL levels [Zador et al., 1993; el-Khatib et al., 1996]. In that study, it was hypothesized that UDP-glucose is utilized by GCS to form GlcCer through its addition to ceramide in diabetic conditions within the kidney. Similarly, we hypothesize that in highly glycolytic cells, such as many cancers, one role of increased glucose uptake is to form UDP-glucose for use by GCS to form GlcCer, in an attempt to deplete ceramide levels and evade apoptosis. It is also plausible that other pathways could play a role in GlcCer formation, such as generation of NADPH for use as a cofactor in de novo ceramide synthesis or fatty acid synthesis for use in the former. The PPP has also been implicated in the transformed phenotype of cancer cells [Buchakjian and Kornbluth, 2010]. Furthermore, glucose-derived pyruvate is utilized by the TCA cycle in transformed cells for production of anaplerotic intermediates such as citrate for fatty acid synthesis [DeBerardinis et al., 2007], a mechanism which would support an increase in overall production sphingolipids, including GlcCer. Future work in this area will focus on the exact substrates elevated in cancer cells in response to increased glucose availability for GlcCer formation, although we speculate that these will include: UDP-glucose, palmitoyl-COA, fatty acids, and NADPH.

Numerous studies have shown that cancer cells present with unique GSL profiles compared to non-neoplastic cells [Hakomori, 1992; Hakomori, 1996; Hakomori and Zhang, 1997; Nohara et al., 1998] Furthermore, elevated GSLs are considered a hallmark of resistance to treatment and cancer aggressiveness [Hakomori, 1996]. GlcCer, the entry point into the synthesis of all higher order complex GSLs (Fig. 1), is synthesized by GCS. As such, GCS has become a target of interest in combatting multidrug resistance (MDR) [Kartal Yandim et al., 2013]. Prior data in our lab showed that PDMP, a ceramide-analog inhibitor of GCS, synergizes with ABT-263, an inhibitor of pro-apoptotic BCL-2 like proteins, in inducing apoptosis in leukemia cells [Casson et al., 2013]. In the present study we showed that both 2-DG and 6-AN, inhibitors of glycolysis and the PPP, respectively, also synergized with ABT-263 in U937 cells. Furthermore, treatment with 2-DG and 6-AN significantly reduced GlcCer levels, which were further decreased upon co-treatment with ABT-263. ABT-263 alone increased the pro-apoptotic lipid ceramide, an effect which was significantly augmented upon addition of 2-DG or 6-AN. Notably, neither 2-DG nor 6-AN increased ceramide levels significantly on their own, indicating that these two metabolic inhibitors act synergistically to augment the effect of ABT-263.

Current standard of care in many cancers focuses on targeting the highly proliferative phenotype of cancer cells with genotoxic drugs such as platinums, anthracyclines, and pyrimidine analogs, among others. However, these therapies are limited by the near inevitability of acquired resistance and metastatic relapse [Rebucci and Michiels, 2013], often of a more aggressive phenotype and poor patient outcome [Dylla et al., 2008; Li et al., 2008; Loges et al., 2009; Milone et al., 2013]. By utilizing therapeutics which do not rely solely on targeting rapid proliferation, that is, genotoxic therapies, but instead which target other intrinsic properties of malignant cells, it may be possible to avoid development of MDR and subsequent relapse. Such is the theory behind the combination of 2-DG and ABT-263, in that this treatment targets two independent weaknesses that are nearly ubiquitous among cancer cells: dependence on aerobic glycolysis and overexpression/dependence on an intracellular target (Fig. 7). It has been shown that the anti-apoptotic subfamily of BCL-2 proteins is overexpressed in a large amount of leukemia subtypes [Placzek et al., 2010; Lagadinou et al., 2013]. The combinatory therapy of 2-DG and ABT-263 has already proven effective in vitro and in vivo in many tumor-based malignancies [Yamaguchi et al., 2011], and we have now shown in the present study that this combination of therapeutics could also serve as an effective treatment option in leukemias.

ACKNOWLEDGEMENTS

Support for these studies was provided by National Institutes of Health NCRR P20 RR17677 COBRE in Lipidomics and Pathobiology pilot project and NIDDK R01 DK093462 to LJS, Start-up funds from the James Graham Brown Cancer Center and the Kosair Pediatric Oncology Research Program to LJB. The contents of this publication do not represent the views of the United States Government. We would like to thank members of the Beverly and Siskind labs for input and technical support.

REFERENCES

Aghaee F, Pirayesh Islamian J, Baradaran B. 2012. Enhanced radiosensitivity and chemosensitivity of breast cancer cells by 2-deoxy-d-glucose in combination therapy. J Breast Cancer 15:141–147.

Bielawski J, Szulc ZM, Hannun YA, Bielawska A. 2006. Simultaneous quantitative analysis of bioactive sphingolipids by high-performance liquid chromatography-tandem mass spectrometry. Methods 39:82–91.

Buchakjian MR, Kornbluth S. 2010. The engine driving the ship: metabolic steering of cell proliferation and death. Nat Rev Mol Cell Biol 11:715–727.

Casson L, Howell L, Mathews LA, Ferrer M, Southall N, Guha R, Keller JM, Thomas C, Siskind LJ, Beverly LJ. 2013. Inhibition of ceramide metabolism sensitizes human leukemia cells to inhibition of BCL2-like proteins. PLoS One 8:e54525.

Chai L, McLaren RP, Byrne A, Chuang WL, Huang Y, Dufault MR, Pacheco J, Madhiwalla S, Zhang X, Zhang M, Teicher BA, Carter K, Cheng SH, Leonard JP, Xiang Y, Vasconcelles M, Goldberg MA, Copeland DP, Klinger KW, Lillie J, Madden SL, Jiang YA. 2011. The chemosensitizing activity of inhibitors of glucosylceramide synthase is mediated primarily through modulation of P-gp function. Int J Oncol 38:701–711.

Chatterjee S, Wei H. 2003. Roles of glycosphingolipids in cell signaling: adhesion, migration, and proliferation. methods in enzymology. In: Yuan CL, Reiko TL, editors. Methods in Enzymology. San Diego: Academic Press. 300–312.

Cori CF, Cori GT. 1925. The carbohydrate metabolism of tumors. I. The free sugar, lactic acid, and glycogen content of malignant tumors. J Biol Chem 64:11–22.

Dang CV. 2012. Links between metabolism and cancer. Genes Dev 26:877–890.

DeBerardinis RJ, Lum JJ, Hatzivassiliou G, Thompson CB. 2008. The biology of cancer: metabolic reprogramming fuels cell growth and proliferation. Cell Metab 7:11–20.

DeBerardinis RJ, Mancuso A, Daikhin E, Nissim I, Yudkoff M, Wehrli S, Thompson CB. 2007. Beyond aerobic glycolysis: transformed cells can engage in glutamine metabolism that exceeds the requirement for protein and nucleotide synthesis. Proc Natl Acad Sci USA 104:19345–19350.

Dwarakanath BS. 2009. Cytotoxicity, radiosensitization, and chemosensitization of tumor cells by 2-deoxy-D-glucose in vitro. J Cancer Res Ther 5 (Suppl1):S27–S31.

Dylla SJ, Beviglia L, Park I-K, Chartier C, Raval J, Ngan L, Pickell K, Aguilar J, Lazetic S, Smith-Berdan S, Clarke MF, Hoey T, Lewicki J, Gurney AL. 2008. Colorectal cancer stem cells are enriched in xenogeneic tumors following chemotherapy. PLoS ONE 3:e2428.

el-Khatib M, Radin NS, Shayman JA. 1996. Glycosphingolipid synthesis and proliferation in a renal cell line grown in high glucose. Am J Physiol – Renal Physiol 270:F476–F484.

Gouaze-Andersson V, Cabot MC. 2006. Glycosphingolipids and drug resistance. Biochim Biophys Acta 1758:2096–2103.

Gouaze-Andersson V, Yu JY, Kreitenberg AJ, Bielawska A, Giuliano AE, Cabot MC. 2007. Ceramide and glucosylceramide upregulate expression of the multidrug resistance gene MDR1 in cancer cells. Biochim Biophys Acta 1771:1407–1417.

Grosch S, Schiffmann S, Geisslinger G. 2012. Chain length-specific properties of ceramides. Prog Lipid Res 51:50–62.

Haimovitz-Friedman A, Kolesnick RN, Fuks Z. 1997. Ceramide signaling in apoptosis. Br Med Bull 53:539–553.

Hakomori S-I. 1992. Functional role of glycosphingolipids in tumor progression. Tohoku J Exp Med 168:211–222.

Hakomori S-I. 1996. Tumor malignancy defined by aberrant glycosylation and sphingo(glyco) lipid metabolism. Cancer Res 56:5309–5318.

Hakomori S-I, Zhang Y. 1997. Glycosphingolipid antigens and cancer therapy. Chem Biol 4:97–104.

Hartmann D, Wegner MS, Wanger RA, Ferreiros N, Schreiber Y, Lucks J, Schiffmann S, Geisslinger G, Grosch S. 2013. The equilibrium between long and very long chain ceramides is important for the fate of the cell and can be influenced by co-expression of CerS. Int J Biochem Cell Biol 45:1195–1203.

Hsu PP, Sabatini DM. 2008. Cancer cell metabolism: warburg and beyond. Cell 134:703–707.

Iida Y, Aoki K, Asakura T, Ueda K, Yanaihara N, Takakura S, Yamada K, Okamoto A, Tanaka T, Ohkawa K. 2012. Hypoxia promotes glycogen synthesis and accumulation in human ovarian clear cell carcinoma. Int J Oncol 40:2122–2130.

Itoh M, Kitano T, Watanabe M, Kondo T, Yabu T, Taguchi Y, Iwai K, Tashima M, Uchiyama T, Okazaki T. 2003. Possible role of ceramide as an indicator of chemoresistance: decrease of the ceramide content via activation of glucosylceramide synthase and sphingomyelin synthase in chemoresistant leukemia. Clin Cancer Res 9:415–423.

Jean-Philippe V, Filippo R. 2003. Role of the ceramide-signaling pathways in ionizing radiation-induced apoptosis. Oncogene 22:8645–8652.

Ji L, Ito M, Zhang G, Hirabayashi Y, Inokuchi J-i, Yamagata T. 1998. Effects of endoglycoceramidase ord-threo-1-phenyl-2-decanoylamino-3-morpholino-1-propanol on glucose uptake, glycolysis, and mitochondrial respiration in HL60 cells. Arch Biochem Biophys 359:107–114.

Jones RG. 2009. The roles, mechanisms, and controversies of autophagy in mammalian biology. F1000 Biol Rep 1:68.

Kartal Yandim M, Apohan E, Baran Y. 2013. Therapeutic potential of targeting ceramide/glucosylceramide pathway in cancer. Cancer Chemother Pharmacol 71:13–20.

Kroemer G, Pouyssegur J. 2008. Tumor cell metabolism: cancer's achilles' heel. Cancer Cell 13:472–482.

Lagadinou ED, Sach A, Callahan K, Rossi RM, Neering SJ, Minhajuddin M, Ashton JM, Pei S, Grose V, O'Dwyer KM, Liesveld JL, Brookes PS, Becker MW, Jordan CT. 2013. BCL-2 inhibition targets oxidative phosphorylation and selectively eradicates quiescent human leukemia stem cells. Cell Stem Cell 12:329–341.

Li X, Lewis MT, Huang J, Gutierrez C, Osborne CK, Wu M-F, Hilsenbeck SG, Pavlick A, Zhang X, Chamness GC, Wong H, Rosen J, Chang JC. 2008. Intrinsic resistance of tumorigenic breast cancer cells to chemotherapy. J Nat Cancer Inst 100:672–679.

Lingwood CA. 2011. Glycosphingolipid functions. Cold Spring Harb Perspect Biol 3.

Liu YY, Hill RA, Li YT. 2013. Ceramide glycosylation catalyzed by glucosylceramide synthase and cancer drug resistance. Adv Cancer Res 117:59–89.

Loges S, Mazzone M, Hohensinner P, Carmeliet P. 2009. Silencing or fueling metastasis with VEGF inhibitors: antiangiogenesis revisited. Cancer Cell 15:167–170.

Lunt SY, Vander Heiden MG. 2011. Aerobic glycolysis: meeting the metabolic requirements of cell proliferation. Ann Rev Cell Dev Biol 27:441–464.

Macheda ML, Rogers S, Best JD. 2005. Molecular and cellular regulation of glucose transporter (GLUT) proteins in cancer. J Cell Physiol 202:654–662.

Maschek G, Savaraj N, Priebe W, Braunschweiger P, Hamilton K, Tidmarsh GF, De Young LR, Lampidis TJ. 2004. 2-Deoxy-d-glucose increases the efficacy of adriamycin and paclitaxel in human osteosarcoma and non-small cell lung cancers in vivo. Cancer Res 64:31–34.

Milone MR, Pucci B, Bruzzese F, Carbone C, Piro G, Costantini S, Capone F, Leone A, Gennaro ED, Caraglia M, Budillon A. 2013. Acquired resistance to zoledronic acid and the parallel acquisition of an aggressive phenotype are mediated by p38-MAP kinase activation in prostate cancer cells. Cell Death Dis 4.

Mullen TD, Spassieva S, Jenkins RW, Kitatani K, Bielawski J, Hannun YA, Obeid LM. 2011. Selective knockdown of ceramide synthases reveals complex interregulation of sphingolipid metabolism. J Lipid Res 52:68–77.

Needleman P, Passonneau JV, Lowry OH. 1968. Distribution of glucose and related metabolites in rat kidney. Am J Physiol 215(3):665–659.

Nohara K, Wang F, Spiegel S. 1998. Glycosphingolipid composition of MDA-MB-231 and MCF-7 human breast cancer cell lines. Breast Cancer Re Treat 48:149–157.

Pedersen PL, Mathupala S, Rempel A, Geschwind JF, Ko YH. 2002. Mitochondrial bound type II hexokinase: a key player in the growth and survival of many cancers and an ideal prospect for therapeutic intervention. Biochim Biophys Acta (BBA) – Bioenergetics 1555:14–20.

Pelicano H, Martin DS, Xu RH, Huang P. 2006. Glycolysis inhibition for anticancer treatment. Oncogene 25:4633–4646.

Pettus BJ, Chalfant CE, Hannun YA. 2002. Ceramide in apoptosis: an overview and current perspectives. Biochim Biophys Acta (BBA) – Mol Cell Biol Lipids 1585:114–125.

Placzek WJ, Wei J, Kitada S, Zhai D, Reed JC, Pellecchia M. 2010. A survey of the anti-apoptotic Bcl-2 subfamily expression in cancer types provides a platform to predict the efficacy of Bcl-2 antagonists in cancer therapy. Cell Death Dis 1.

Presley J, Mayor S, Dunn K, Johnson L, McGraw T, Maxfield F. 1993. The End2 mutation in CHO cells slows the exit of transferrin receptors from the recycling compartment but bulk membrane recycling is unaffected. J Cell Biol 122:1231–1241.

Rathmell JC, Fox CJ, Plas DR, Hammerman PS, Cinalli RM, Thompson CB. 2003. Akt-directed glucose metabolism can prevent bax conformation change and promote growth factor-independent survival. Mol Cell Biol 23:7315–7328.

Rebucci M, Michiels C. 2013. Molecular aspects of cancer cell resistance to chemotherapy. Biochem Pharmacol 85:1219–1226.

Siskind LJ, Mullen TD, Romero Rosales, Clarke K, Hernandez-Corbacho CJ, Edinger MJ, Obeid AL. 2010. The BCL-2 protein BAK is required for long-chain ceramide generation during apoptosis. J Biol Chem 285:11818–11826.

Spiro MJ. 1984. Effect of diabetes on the sugar nucleotides in several tissues of the rat. Diabetologia 26:70–75.

Tsavachidou D, Li Y, Guo H, Liu W, Jonasch E, Tamboli P, Mills GB. 2010. Glycogen metabolism provides nutritional support to renal cancer cells under conditions of stress and may serve as a marker of response to antiangiogenic therapy with bevacizumab. AACR Meeting Abstracts.

Vander Heiden MG, Cantley LC, Thompson CB. 2009. Understanding the Warburg effect: the metabolic requirements of cell proliferation. Science 324:1029–1033.

Warburg O. 1956. On the origin of cancer cells. Science (New York, N.Y.) 123:309–314.

Yamaguchi R, Janssen E, Perkins G, Ellisman M, Kitada S, Reed JC. 2011. Efficient elimination of cancer cells by deoxyglucose-ABT-263/737 combination therapy. PLoS ONE 6:e24102.

Zador IZ, Deshmukh GD, Kunkel R, Johnson K, Radin NS, Shayman JA. 1993. A role for glycosphingolipid accumulation in the renal hypertrophy of streptozotocin-induced diabetes mellitus. J Clin Invest 91: 797–803.

Zhao H, Przybylska M, Wu I-H, Zhang J, Siegel C, Komarnitsky S, Yew NS, Cheng SH. 2007. Inhibiting glycosphingolipid synthesis improves glycemic control and insulin sensitivity in animal models of type 2 diabetes. Diabetes 56:1210–1218.